Vol. 45, No. 1 (2023) 12-33, DOI: 10.24874/ti.1381.09.22.01

Tribology in Industry

www.tribology.rs

REVIEW

A Review on Modeling and Stability Aspects of Gas Foil Bearing Supported Rotors

Debanshu S. Khamari[a,*], Jitesh Kumar[a] , Suraj K. Behera[a]

[a]*National Institute of Technology Rourkela, Odisha, India.*

Keywords:

Gas foil bearings
Simple elastic foundation model
Coupled fluid structure model
Nonlinear rotordynamics
Subsynchronous motions

* Corresponding author:

Debanshu S. Khamari
E-mail: debanshushekhar@gmail.com

Received: 29 September 2022
Revised: 16 November 2022
Accepted: 13 January 2023

A B S T R A C T

Gas foil bearing rotor (GFBR) systems have received significant interest in the field of rotordynamics and vibration analysis. GFBR systems have a wide range of high-speed turbomachinery applications. Due to the high speed, these machines are susceptible to rigorous vibration and instability. Gas foil bearings instigate large amplitude of vibrations at startup and shut down and severe subsynchronous motions during high-speed operations. Over the years, numerous work has been done in the field of high-speed rotors supported on gas foil bearings. Significant improvement has been observed in the stability and feasibility of the GFBR systems. However, accurate model predictions of gas foil bearing still remain a challenge for its widespread usage in high-speed turbomachinery. A comprehensive review needs to be done to study the previous work and pave the way for future research. The current review is majorly divided into three sections. Firstly, various models used for the performance prediction of gas foil bearings are compiled. After that, major causes of instability that manifest during the experiments and practice with gas foil bearing supported rotors is illustrated. Lastly, the developmental attempts made to inhibit the instability is summarised. This paper presents an overall picture of the current engineering scenario and future prospects of the GFBR systems.

1. INTRODUCTION

Gas foil bearings (GFBs) are particularly valuable when they support high-speed rotors that are preferably lightly loaded [1]. GFBs have been widely adopted in various high-speed applications, such as air cycle machines [2,3], turbocompressors [4,5], turbogenerators [6,7], turbochargers [8,9], gas turbine engines [10,11], turboexpanders [12,13] etc. as shown in Fig. 1. In the case of the considered type of bearings, the rotational speed can be as high as tens or hundreds of krpm (thousands of revolutions per minute) [14]. GFBs basically consist of a bearing base over which a spring-like compliant structure is placed to tailor the stiffness and damping. The main advantage of using foil bearing is that it provides substantial damping when compared to thin air film during operation. The smooth top foil is placed over a compliant structure to overcome

frictional losses at the start and stop of the rotor. The fluid film caused due to the rotating action between the rotor and top foil is responsible for the generation of hydrodynamic pressure, which is responsible for carrying the unbalance load generated in the system.

The bump and top foil are manufactured using different methods [15]. One of the methods is to use the forming process on the thin sheet of material to give correct contours. Another method is to move the thin sheet within two meshing spur gears. However, current technologies involve the use of CNC machines and additive manufacturing methods to fabricate the GFBs. Conventional GFBs provide excellent dynamic stability but low load-carrying capacity owing to their compliant nature. So, researchers have been working on innovative GFB design and manufacturing to improve the dynamic performance and increase the load-carrying capacity. Various novel GFBs which have been manufactured and tested include lobbed three-pad GFB [16], GFB with compression springs [17], active GFB [18], metal-mesh GFB [19,20], lobed GFB [21,22], Shimmed GFB [23] and GFB with shape memory alloy (SMA) springs [24].

The use of GFBs in turbomachinery requires the model to be able to provide accurate performance predictions. GFBs instigate subsynchronous motions, which is the major cause of failure in gas foil bearing supported rotors. In order to avoid this instability, it is vital to investigate the vibration generation sources. Moreover, the size correlation between the subsynchronous motions and the GFBs is needed to be studied for the safe functioning of the rotor. Establishing a nonlinear dynamic model that accounts for the shaft motions, gas film and fluid-structure interactions still remain a challenge for researchers around the globe. Till now, some review papers related to the design and development of foil bearings have been reported [25,26]. In addition, the work presented by DellaCorte et al. [27-30] on the progress and challenges of oil-free turbomachinery is admirable. After going through all these reviews, it is observed that the stability characteristics are enhanced with the use of gas foil bearings that could not be attained in the system supported by oil-lubricated bearings. As far as the author's understanding, no review paper on the stability aspects of high-speed rotors considering gas foil bearings has been reported yet.

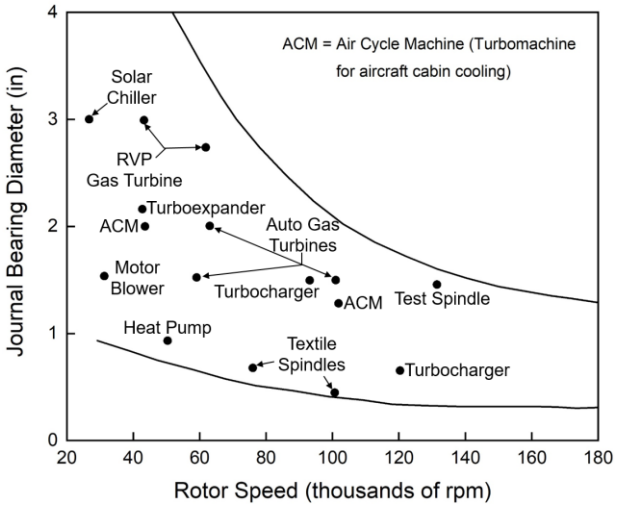

Fig. 1. High-speed applications for GFBs [4].

This paper mainly reviews the static and dynamic performance of GFBs through various predictive models and the recent progress on response measurements and analysis of GFBR systems. Major findings from the research carried out to predict the performance of GFBs is presented in Table 1. The dynamics of gas foil bearing supported rotors is summarized in Table 2. The emphasis of this review is on compliant gas foil bearing supported rotors. The overall structure of this paper is organized as follows: In Section 2, various models for gas foil bearing performance prediction is reviewed. Section 3 illustrates the causes of instability in GFBR systems. In Section 4, various factors that are useful to overcome the instability in gas foil bearing supported rotors are discussed. Discussions and future prospects are given in Section 5, followed by conclusions in Section 6.

2. COMPUTATIONAL MODELS FOR GAS FOIL BEARING PERFORMANCE PREDICTION

The use of GFBs in high-speed turbomachinery necessitates precise performance predictions based on credible test data. GFBs must be able to withstand the load and provide sufficient stiffness and damping, as low dynamic coefficients result in instability in rotor-bearing systems. It is also important to develop a robust computer program with the complications of model convergence and high processing durations. There are two aspects to GFB modeling. One is the fluid aspect and another is the structural aspect. The fluid aspect is modeled by Reynolds equation [31]. It is solved mainly by

various numerical methods, viz. finite element (FE), finite difference (FD) and control volume (CV) method. The structural part is modeled by the FE method and an analytical method based upon strength of materials (spring, mass, link, friction pair etc.). Most foil bearing models now use a kind of copulated hydrodynamics-structural approach. However, combining the models might result in convergence problems and extended processing durations. Moreover, there is a persistent need to improve computation time in the many numerical analyses performed nowadays. There needs to be a balance between the computational effort and the accuracy of the chosen GFB model. Therefore, it is vital to choose a reliable validated numerical method that accounts for both the fluid and structural characteristics of the GFB. A detailed review of the models is presented hereafter.

2.1 Simple elastic foundation model

Heshmat et al. [32] first incorporated the flexibility of the foil in the gas foil journal bearing (GFJB) model by introducing a linear elastic displacement as a function of fluid film pressure. The analytical expression for foil flexibility was given by Walowit et al. [33]. This approach to modeling is known as the simple elastic foundation model (SEFM). Small pressure perturbations are introduced into the Reynolds equation. The discretized equations are then solved using the Newton-Raphson approach. Different design parameters such as eccentricity ratio and compliance are varied, and their influence on the load capacity and film thickness are identified. It is observed that with the increase in the compliance of the bearing, the load-carrying capacity decreases and the film thickness increases. Therefore, at low loads, it is preferable to use high compliance bearings. The collinear and cross-coupled stiffness is also calculated, which are observed to settle down with the increase of eccentricity. Subsequently, Heshmat et al. [34] estimated the SEFM stiffness coefficients for the gas foil thrust bearing (GFTB) using the FD approach. It is found that there is a nominal change in the stiffness coefficients with the increase of load on the bearing. Generally, in the FD method, the Taylor series is used to expand the governing Reynolds equation. The accuracy of the solution depends on the number of higher-order terms. The solution starts after splitting the bearing surface into a number of grids. The equations are solved by discretization followed by an iterative method to determine the pressure at each point on the grid. This method is often used for GFB models as it can solve higher-order schemes. However, it cannot accumulate non-regular solutions and is only feasible for structured models. Also, proper integration and approximation techniques must be used for lesser computational efforts and faster convergence of the FD formulation. Peng and Carpino [35] improved the SEFM by including a mechanical loss factor, which allowed the SEFM to accumulate dissipative contributions from the foil. The influence of various bearing parameters such as bearing number, compliance number and eccentricity ratio on the stiffness and damping was investigated. The analytical results are compared with that of Heshmat et al. [32], which revealed minor differences but assured higher accuracy. The stiffness coefficients are found to rise as the bearing number rises and decline as the bearing compliance rises. This is because, at low speeds, the bearing compliance is mostly dependent on the lubricant film, which is comparatively softer in comparison to the stiffness of the elastic foundation. The damping coefficients, on the other hand, progressively grow with the bearing number, reach a maximum, and then decline. The reason being the gas film which is relatively rigid at high speeds, preventing any energy loss in the gas film. The SEFM was further extended by several authors [36-39] to link it to the analytical perturbation method.

The drawback of the SEFM is that it neglects the top foil sagging, stiffening effect, bump interactions and friction forces. Iordanoff [40] addressed this problem to some extent by including the stiffening effect of the Coulomb friction, and Peng et al. [41] included the damping caused by the Coulomb friction in the SEFM. Subsequently, Larsen and Santos [42] incorporated the flexibility of the compliant foil structure in the model. The FE formulations of the nonlinear Reynolds equation was derived for a three-pad GFJB. The convergence is achieved by using the Newton-like method and the Successive Under Relaxation method. In comparison, the former is found to have a faster convergence than the latter. The deflection of the bumps and top foil sagging effect are considered to estimate the pressure profiles. Significant influence of the sagging effect on the pressure profile is observed, particularly on the second pad. Larsen et al. [43]

further developed the SEFM by including the effect of Coulomb damping. The dynamics of the bump foil strips and the contact points of the GFJB are considered for the modeling. Coulomb damping is found to be proportional to its confined area in the hysteresis loops. It is observed that higher confined area at any vertical displacement leads to higher Coulomb damping and in turn making the stiffness more nonlinear at that point.

2.2 Coupled fluid-structure model

As suggested by the above literature, the friction effects generated in the GFB are the major cause behind the nonlinear behavior of the foil structures. Due to the friction, added damping is induced in the compliant structure, which contributes to the fluid film damping. Coupled fluid-structure models can be divided into two parts. One is the analytical model in which the compliant structure is approximated by simple springs. Other is the detailed model where the compliant structure is accurately modeled by mathematical principles. One of the earliest work on analytical model was carried out by Ku et al. [44-46], which takes into account the forces of bump contact, friction between bearing components, variable loading conditions and local interaction forces. The technique anticipates substantial variations in stiffness between bumps by calculating the number of bumps that are pinned owing to friction. The findings demonstrate that lower friction coefficients result in softer bumps with more deflection in both radial and axial directions. Also, an increase in the friction coefficients at the contact surface results in Coulomb damping and increased stiffness. Later, the interaction forces between the bump foil and top foil were considered to estimate the deformation characteristics. The presence of changing stiffness in the bump foil strip was verified and the dynamic coefficients are calculated for the GFJB [47]. The results for the structural stiffness and damping are found to agree well with the experimental results [48]. In the case of GFBs, Coulomb friction accounts for the coupled thin air film and the frictional motion of the foil structure. Small sinusoidal perturbations of the journal are taken and the effect of Coulomb friction is considered to predict the dynamic coefficients [49]. The FE method is utilized to simulate the bump motion and the nonlinearity is handled using a direct implicit integration methodology. The reason for using the FE method is that it can be used to model any complex-shaped geometry using the element formulation of the Reynolds equation. However, the FE method requires more mathematics than any other method, which might increase the computational time. After that, Lee et al. [50] utilized four-node elements to obtain the pressure and dynamic coefficients. The time marching (TM) method was used to obtain the dynamic response. It is found that as the coefficient of friction rises, the damping nature of the air film becomes more prevalent than the bump foil due to stiffer bump foil. The resonant amplitude was found to be minimum at the optimum value of the friction coefficient. Friction forces are also influenced by foil materials, displacement, and relative velocity of contact surfaces and greatly affect the dynamic characteristics of GFBs [51]. Hysteretic behavior of the friction between the bump and the contact surfaces is another aspect that is investigated using an analytical structural model [52]. The result shows that there is a significant effect of hysteresis on the eccentricity ratio and applied load.

Interaction forces between bumps and friction forces at contact surfaces are other important factors that must be considered to represent the complete structural behavior of the GFB. Fatu and Arghir [53] carried out a structural analysis of foil bearing by considering foil structure as a network of interacting springs. However, the connection between the top foil and the bump foil, as well as the connection between the bump foil and the bearing base are assumed to be closed in the model. This assumption reduces the computing effort but compromises the accuracy of the model as the contact state might shift from close to loose. Hence a new model was developed [54] by taking into account the effect of mainly three close or loose contacts: the contact between the rotor and top foil, the contact between the top foil and bump foil, and the contact between the bump foil and bearing base. Hryniewicz et al. [55] proposed another analytical model which predicts the structural response of bump and top foil under arbitrary pressure loading conditions. The 2D analytical model developed took into account bearing geometry, bump interaction and frictional forces. The proposed model was compared to existing models in the literature. A second FE model was also created for further

verification. The two models were thus used to illustrate the deflection and developed stresses at the bumps. The first bump is observed to have the largest deflection and stress as it's one end is free and neighboring bumps are not available to stiffen its structure. Contrarily, the smallest level of deflection and stress is observed at the pinned end. Later, the stiffness of bumps and internal forces within the foil structure is included in the structural model [56]. Bumps are represented by rigid links and horizontally spaced springs. A FE shell model is utilized to calculate the top foil deflection. The influence of interaction forces and friction forces inside the foil structure is also estimated. Then, the structural stiffness is evaluated by applying Castigliano's theorem. TM method was used to analyse the dynamic response. It was observed that the subsynchronous motions start to disappear above a certain threshold of imbalance eccentricity. Le Lez et al. [57] observed that bump interaction must be considered in the structural model; otherwise, bump flexibility is overestimated. They constructed a three dimensional (3D) model for the foil structure that considers the bump interaction as well as top foil deflection. Subsequently, an NDOF model is developed in which the foil structure is replaced by equivalent nonlinear springs [58]. This multi degree of freedom (DOF) system can accommodate the strips constituted of a higher number of bumps. TM method was adopted to study the response. The vertical displacements of the top of the bumps and load distributions are determined and compared with the FE simulations for the structure of ten bumps. Marginal differences in the results validate the accuracy of the model. The comparative response obtained for a single bump case is observed to be quite distorted, which demonstrates the importance of bump interactions in the model. In addition to the interaction forces at the contact surfaces, the effect of lateral deflection of the flat segment between bumps was taken into account in the model by Gad et al. [59]. This approach enables the fluid film thickness to be calculated using the deflection induced by the structural model. The fluid flow is represented in cylindrical dimensions using the compressible Reynolds equation. The Newton-Raphson technique is utilized to linearize the nonlinear equations, and a tri-diagonal matrix algorithm is used to solve them repeatedly. Flexible boundary conditions at bump ends are also taken into account by the model. This model's deflection is compared to that provided by prior analytical models [55-58]. The neglection of flat segment deflection is shown to overstate the stiffness. Later, Gad et al. [60] used a similar structural model and incorporated the effect of centrifugal forces in the gas film. The model was used to predict the static and dynamic characteristics of a second generation GFTB. In the subsequent work, Gad et al. [61] provided different bump foil designs to tailor the stiffness and investigated its influence on the static characteristics of the GFTB.

The bump foil structure is primarily modeled in the preceding literature using analytical methods. There is numerous work based on detailed structural models obtained through mathematical models and later discretized using FE, FD and CV method. Carpino et al. [62] carried out detailed structural modeling of a GFJB by incorporating the fluid flow effects and structural deflections into a single FE. A modified forward iteration approach is used to solve the discretized equations. Later, a fully coupled FE model is presented, which provides a distinct advantage of varying the extensive structural and operating parameters [63]. The resulting nonlinear equations are deduced utilizing the Newton-Raphson method. Pressure profile, minimum film thickness and load capacity are calculated for a GFJB. The results depict a sufficiently fine mesh in the exit region of the gas film, which prevents the undulations occurring in the pressure and film thickness. Carpino and Talmage [64] introduced a model in which the film thickness, deflection and pressure are perturbed using the FE method to obtain the dynamic coefficients. Both structural and fluid effects are incorporated to formulate the model. The corrugated sub foil is modeled as a continuous structure, and the Coulomb friction is considered as viscous friction. However, the effect of foil flexibility is not given due importance. They also tested the influence of journal misalignment on the stability of the GFJB [65,66]. The membrane stress and elastic foundation characteristics of the bearing are reported in the work. Later, Osmanski et al. [67] developed a fully coupled FE model of a GFJB, which incorporated the mass of the foils and the dynamic friction. The inclusion of mass dependency was a necessary implementation to the model. However, including the dynamic friction resulted in an inaccurate prediction of the imbalance response of the model. Moreover,

excessive top foil sagging was observed due to the omission of curvature effects and membrane forces. Unstructured grids are solved using the CV method. Bhore et al. [68,69] used the CV method for a GFB model using a two-dimensional grid for discretization. Gauss-Siedel iterative scheme is used to solve the discretized equations. The pressure is integrated using the Simpsons rule, and the load-carrying capacity is calculated. The Reynolds equation is coupled with the rotor equation of motion to study the nonlinear dynamics of the rotor via bifurcation diagrams and Poincare maps. Various operating parameters such as unbalance, speed and eccentricity are also taken into account to study the nonlinear behavior of the journal center. Although the CV method is straightforward and commands less computational effort, it is not often used for GFB modeling because of the difficulty in solving higher-order schemes. The influence of slip-flow effect on the hydrodynamics of the GFBs has been investigated. Shahdhaar et al. [70] included the slip-flow phenomenon in the GFJB model using the FD method. It was found that there was a decrease in the load-carrying capacity and an increase in the attitude angle with the inclusion of the slip-flow effect. Later, Kumar et al. [71] considered the first-order velocity slip in the model and presented a comparison between the slip and no-slip conditions for the GFJB. It was found that the load-carrying capacity for slip flow was lower than that for the no-slip flow as there was lesser generation of hydrodynamic pressure. A negligible effect was observed in the parameters like torque and power loss due to the slip flow. Subsequently, Kumar et al. [72] incorporated the slip-flow effect in in a GFTB model and presented a modified Reynolds equation with the first-order slip condition. It was observed that the traditional Reynolds equation has a bias towards overestimating the load-carrying capacity of the GFTB. Different analytical methods have been used to evaluate the static and dynamic characteristics of the GFB. It is important to measure the level of influence of each design variable on the static and dynamic characteristics. Khamari et al. [73] estimated the influence and sensitivity of length-to-diameter ratio, eccentricity ratio, bearing number, whirl ratio, and bearing compliance on the stiffness and damping of the GFJB. It was observed that the eccentricity ratio was the most effective parameter, whereas the whirl ratio had the least effect on the dynamic coefficients. Findings also showed that the normalized stiffness rises with the bearing number and falls with rising bearing compliance, whereas the normalized damping exhibits the opposite behavior. In addition, when the speed increases, stiffness coefficients tend to rise while damping coefficients fall. Later, Kumar et al. [74] deduced the most effective parameters on the load-carrying capacity of a GFB. It was found that minimum film thickness, angular extent ratio at wedging, the angular extent of the thrust pad, and rotating speed have a substantial influence on load capacity.

The movement of the rotor and the top foil generates a wedge of air that assists the rotor. The top foil gets deflected in response to the pressure profile developed in the fluid film. So the deflection of the top foil directly influences the fluid-structure analysis [75]. Lee et al. [76] took into consideration the top foil deflection in the GFB model and predicted load capacity, minimum film thickness and attitude angle. The results are compared with that of the models not considering the top foil deflection. It is observed that the results considering the effect of the top foil show a more exact solution than the results of those effects not considered. The effect of top foil largely accounts for the performance of foil bearings. An advanced FE method is developed by coupling the top foil deformations to bump deflections and the dynamics of the gas film simultaneously [77,78]. The sagging effect of the top foil is also included in the model. The performance of the model is predicted by comparing previous experimental test data with a SEFM, one-(1D) and two dimensional (2D) FE top foil models. The DOF of 1D model is represented as transverse deflections and rotations with generalized displacements. The film thickness is calculated and observed to agree well with previous experimental test data [79] along the zone of minimum film thickness. In the 2D model, the top foil is represented as a flat shell supported on axially distributed linear springs. The stiffness coefficients are calculated for the models. The direct stiffness coefficients tend to increase with the excitation frequency implying the hardening effect of the gas film. The SFEM prediction shows the largest direct stiffness coefficients, whereas the 1D and 2D model tend to give the smaller values. The damping coefficients are also calculated for the models and tend to show similar behavior as that of the

stiffness coefficients. Subsequently, Lee et al. [80] used a 3D foil structural model to calculate the foil deflection. The pressure profile is estimated using four node rectangular elements with linear shape functions. Film thickness is calculated for various top foil thicknesses. It is observed that the use of the thinnest top foil results in the least minimum film thickness. The results show that thinner top foil leads to severe foil structure deflection and a significant decrease in the load-carrying capacity. Later, Xu et al. [81] modeled the top foil as a 1D curved beam to obtain the minimum film thickness and attitude angle. The results are compared with 1D FE models and the SEFM. The variation of minimum film thickness is also compared with the test data [79]. The results agree well along the zone of minimum film thickness. Subsequently, a 2D plate top foil model is proposed based on the thick plate theory to study the shear stiffness effects of a GFB [82]. A sagging effect is observed at the zone of minimum film thickness which is due to the softness of the top foil in adjacent bumps. The minimum film thickness and attitude angle of the proposed model is compared with the previous 1D and 2D FE top foil model [77]. The results depict a good agreement in the data and indicate the necessity of shear stiffness in the model. Nielsen et al. [83] investigated the top foil sagging effect of the bearing on the rotor's transient and steady-state response. TM method was used to obtain the dynamic response. Some unsupported areas are created in the GFB by removing some bumps. It is observed that shallow pockets are produced in unsupported areas due to the sagging effect of the top foil. As a result of which, subharmonic motions are significantly reduced when the unsupported area is placed properly. The results also depict visible sagging at the minimum film thickness profiles for partially supported top foil in the GFB. Clearly, the use of bump foil which acts as an elastic cushion and complaint the top foil provides adequate stability and reliability. There is a relationship between the dynamics of the gas film, foil structure, and the vibration characteristics of the rotor, which is investigated to study the instability in rotors. The overall stiffness of the GFB consists of the gas film and foil structure stiffness. The stiffness governs the characteristics of subsynchronous motions in GFBR systems. Subsynchronous motions instigate instability and are the major cause of failure in GFBR systems. This aspect is reviewed in the following section.

3. STABILITY CHARACTERISTICS OF GAS FOIL BEARING ROTOR SYSTEMS

Nonlinear characteristics of the GFBs are responsible for the nonlinear behavior of the rotor. This nonlinearity instigates significant subsynchronous motions, which are the major cause of instability in GFBR systems. Experiments and analysis suggest that the subsynchronous motions are strongly related to the gas film and foil structure of the GFB. The following summarises research efforts to obtain an understanding of the major causes of instability in GFBR systems.

Heshmat et al. [84] introduced a concept called 'lobbing effect' into a three pad GFB by using a variable stiffness gradient of the foil. The lobbing effect is created due to the pressure generated in the GFB. This is done by varying the pitch of the bump from the trailing edge to the leading edge of the bearing. This phenomenon was observed through the load deflection test in which the stiffness is found to be increasing towards the trailing edge. The pads are driven outward with the increase in speed which in turn generates a converging wedge in the bearing. This lobbing effect becomes more prominent with the increase in speed and results in improved stability of the GFB. The three pad GFB was able to achieve a stable operating speed of 120,000 rpm. Various level of unbalance was also introduced into the GFB, and the unbalance response was studied. It was observed that the onset speed of instability (OSI) decreases with the increasing unbalance mass resulting in significant subsynchronous motions in the GFB. Subsequently, Heshmat et al. [85] presented a novel foil bearing with a multilayer bump foil arrangement for high-speed and load capacity applications. The rubbing action between the bump foil and top foil provided an improved Coulomb damping. The GFBR system was able to attain a breakthrough speed of 132,000 rpm and a load capacity of 673.5 kPa. Coast down test was conducted, and the rotor response was studied. Subsynchronous motions were observed at both principal resonant frequency and rigid body natural frequency. Orbit plots indicate that the orbital displacement gradually increases and then decreases with the rise of rotor speed. The rotor was stable at the maximum operating speed of 132,000 rpm with relatively lesser peak-to-peak amplitudes. Later, Heshmat [86] tested three

different types of GFB with different stiffness levels in a rotor-bearing system. First bearing had single layer of bump foil. Second bearing had multiple layer of bump foils and third one had multiple layer of bump foil with Cu coating. The bearing damping coefficients were calculated from the peak hold amplitude data during rotor run up and coast down. Waterfall plot was obtained and coast down response was recorded. The system response was synchronous with the rotating speed prior to the commencement of the bending mode. Subsynchronous motions with a frequency that corresponds to a rigid body mode natural frequency start to appear while passing through the bending mode critical speed. The rotordynamic performance of the three bearings is found to be similar in nature.

Linear frequency domain simulation is not sufficient for the stability analysis of the GFBs. Nonlinear TM simulations are required for the complete information on the bearing stability [16]. Larsen et al. [87] compared the stability of the GFB using two primary methods (perturbation method and TM method). One in the linear frequency domain approach and the other in the nonlinear time domain approach. The methods are used to predict the OSI with varying structural stiffness of the foil. The time domain approach is used to predict the response of the GFBR system. It is observed that the OSI goes on increasing as the foil structural stiffness decreases for both the time domain and frequency domain approach. Severe instability in rotor orbits also depicts the sensitivity to foil stiffness. The results of stability analysis from the perturbation method were determined to be incorrect when compared to that of the TM method. The TM method was found to be more computationally expensive. This is because the TM method demands numerical integration with extremely precise time increments. Different types of perturbation methods were also used by Osmanski et al. [88] for the analysis of the compliance level of the GFB. It is verified that softer foil results in higher OSI, and increasing the stiffness makes the bearing rigid and unstable. Zhou et al. [89] investigated the stability of a GFTB supported gas turbine rotor. Orbits and vibration spectrum were obtained at 125,413 rpm. Orbits were found to be elliptical, and the spectrum of vibration was found to be sinusoidal in nature. A high amplitude of synchronous motion was observed in the waterfall plot with small amplitude of subsynchronous vibrations. The rotor was found to be stable up to the rotating speed with a small amplitude of vibration in radial directions. Axial direction vibration amplitude was observed to be nominal denoting stable operations of the GFBR system at high speed. Kim et al. [90] estimated the performance of a 75 KW turbo blower rotor supported on GFBs at a rated speed of 30,000 rpm. Subsynchronous motions are observed from 90 Hz to 120 Hz. A comprehensive small amplitude excitation frequency is found above the rotor speed, which signifies rub condition between the rotor and foil bearing. An inspection of the foil showed slight rubbing on the GFJB top foils and notable wear on the GFTB top foil. It implied that GFTB has a lower load capacity as it failed to support the unbalanced axial force. After using a larger radius GFTB of 83 mm for the enhanced load capacity and increased loading area, a significant improvement in the rotor performance is observed with dominant synchronous motions up to the rated speed. Song et al. [17] presented a new type of GFB in which compression springs were used instead of bump foils. The effect of this elastic foundation on the stability of the rotor was investigated. The stiffness and structural loss factor were measured, and the TM method was used to calculate the coast down response and orbits of the GFBR system up to a speed of 16,000 rpm. It is observed the damping provided by the elastic foundation was sufficient enough to cross the critical speed of the system effectively. However, the system was observed to be highly unstable at the OSI of 14,400 rpm. The orbits were also observed to be distorted around 14,400 rpm, denoting the instability of the GFBR system at this speed. The authors note the importance of structural damping in preventing subsynchronous vibrations. The benefits of including structural damping in the GFB are validated by a computational viscous model [91]. TM method was used to analyze the response of the GFBR system. It is observed that the stability speed limit of the bearing considerably increases by additional structural damping. A comparison with similar rigid bearings depicted that the compliant GFBs with no structural damping are not as stable as the rigid bearings. Walton et al. [92] designed two test rigs for the stability analysis of an air cycle machine and a cryogenic turboexpander supported on GFBs. The air cycle machine was operated at a speed of 100,000 rpm.

The stability map was obtained which indicates the positive logarithmic decrement values for the stable operation of the system. The cryogenic turboexpander rotor was supported by two GFJB and a GFTB. The FFT plots were obtained at the turbine and compressor sides. The rotational speed of the GFBR system was found to be 61,440 rpm. The compressor end vibrations are found to be a bit weaker than the turbine end. Both side vibration spectrums contained synchronous motions with small amplitude of subsynchronous motions. The coast down response indicated the second mode critical speed with a peak at 13,400 rpm. The angular location of the bearing was varied, and its effect on the stability of the GFBR system was studied. The coast down response and FFT plots showed that the rotor remained stable throughout the operating speed irrespective of the varying angular position of the bearing. Subsequently, Walton et al. [93] conducted the experimental investigation of a turbocharger rotor supported on pair of GFJB and a GFTB. The stability of the system was tested up to an operating speed of 150,000 rpm. FFT plots at both the drive and non-drive end showed a clear peak at the operating speed. The operation of the rotor was smooth throughout the speed with small amplitude of subsynchronous motions. Dynamic load tests were conducted to study the GFBR system response to shock loading. The recorded vibration spectrum shows the orbit size to be small after the shock test. Coast down response of the rotor denoted stable operation of the system with dominating synchronous motions. The nature of the gas film and the foil structure deformations affect the stiffness of the GFB, which in turn governs the characteristics of the subsynchronous motions. These subsynchronous motions are basically whirl and whip vibrations instigated by the GFB. Guo et al. [94] analyzed the effect of overall GFBR system dynamic stiffness on the subsynchronous vibration with respect to the rigid behavior of the rotor and the stiffness of the GFB. The subsynchronous vibrations from the test data exhibit a strong correlation with the results from the FE simulation. It is observed that the rotor eccentricity ratio appears to rise as the rotational speed rises, and the foil structure gradually becomes more flexible than the gas film. So the foil structure stiffness dominates the overall system stiffness. As the number of effective bumps is limited, the system stiffness becomes almost constant, resulting in constant whip frequency. However, as the speed starts to reduce, gas film stiffness commands over the system stiffness. As a result, whirl frequency is observed at low rotational speed due to the excitation generated by the tangential force component of the gas film. Similar characteristics are observed when a comparative investigation is conducted between the predictions from the FE model and measured test data of the GFBR system [95]. A significant deviation in the synchronous amplitudes is observed at low rotor speeds as the GFB stiffness departs from the rigid gas film. Also, at low rotor speeds, the diminishing effects of whip frequency are observed, and with the increase of speed, both the severity and magnitude of whip amplitude are found to be increasing. The increase in whip frequency due to increased system stiffness was also observed with an active bump foil bearing [18,96]. The predictions demonstrate that the whip motion is largely determined by the foil structure properties and relates to the system's low modal frequency, which is excited by the gas film. However, in the oil-bearing rotor system, the shaft stiffness dominates the oil film stiffness [97]. The oil film stiffness rises only when the rotor speed is significantly high. Also, the whip vibrations in the oil-bearing rotor system are related to the excitation of bending shaft mode compared to that of the bump foil structure in the GFBR system. Moreover, the whip vibration amplitudes in GFBR systems are much larger than the cylindrical synchronous vibrations where as in the case of oil-bearing rotors, the synchronous vibrations present relatively small amplitudes than the conical whip vibrations. It is vital to control the subsynchronous motions as these are the major cause of failure in GFBR systems. The work carried out on the controllable factors to overcome the instability in GFBR systems is presented hereafter.

4. INFLUENTIAL FACTORS TO OVERCOME THE INSTABILITY IN GAS FOIL BEARING ROTOR SYSTEMS

Subsynchronous vibrations in rotors supported by GFBs are not rare. Many developmental attempts have been made in an attempt to correct or control these unwanted vibrations. In what follows, we review the critical factors that are beneficial for the stability of the gas foil bearing supported rotors.

4.1 Mechanical preload

An assembly preload of top and bump foil is often introduced in GFBs, which leads to a contact of top foil and rotor in case of a non-rotating, perfectly aligned rotor. As a consequence of the assembly preload, the stiffness of the bearing, the overall bearing structural damping, and the response of the rotor are affected. Sim et al. [21, 22] investigated the influence of mechanical preload on the onset speed of subsynchronous (OSS) motion and OSI of a turbocharger rotor supported on lobed GFB. It is observed that the speed of initiation of subsynchronous motions goes on increasing with the increasing mechanical preload. The increase in the system's natural frequency implies strong wedge effects in the lobed GFB clearance profiles and improved rotordynamic performance. Also, the rise in OSI confirms the stabilizing effects of increasing mechanical preload in lobed GFBs. A rotordynamic analysis was conducted using a FE model of the rotor. The critical speeds for conical mode, cylindrical mode, and first bending mode are predicted with and without housing vibrations. The nature of rotor vibration modes with housing is observed to be identical to those of vibrations without housing. The beneficial effects of increasing mechanical preload on the OSS motions are also noticed with a turbocharger rotor supported on three-pad GFBs [98]. Waterfall plots are obtained for one pad and three-pad GFJB with load on pad and load between pad conditions. The occurrence of significant synchronous motions for load on pad one pad GFJB depicts the positive effects of pad split on the performance of the GFB. Moreover, for load between pad three-pad GFJB, small subsynchronous motions are observed at 180 Hz frequency. However, for load on pad three-pad GFJB, no subsynchronous motions are found up to a rotating speed of 93,000 rpm, implying comparatively better performance. The FE model of the rotor is used to predict the natural frequency and mode shapes. It is observed that as the rotor speed rises, the rigid mode critical speeds drop at lower speeds owing to rotor migration to the bearing centre and increase at higher speeds due to film stiffening effects. The predictions for peak amplitudes and critical speeds are found to agree well with the experimental data. A typical industrial practice is to insert metal shims underneath bump strips to induce mechanical preload at a very low cost as shown in Fig. 2 [99]. The preload generates a hydrodynamic wedge which creates more pressure supporting higher loads. It is observed that the amplitude of subsynchronous motions significantly decreases with the shimmed GFB. There is also an increase in the threshold speed of subsynchronous motions with the increase in the mechanical preload.

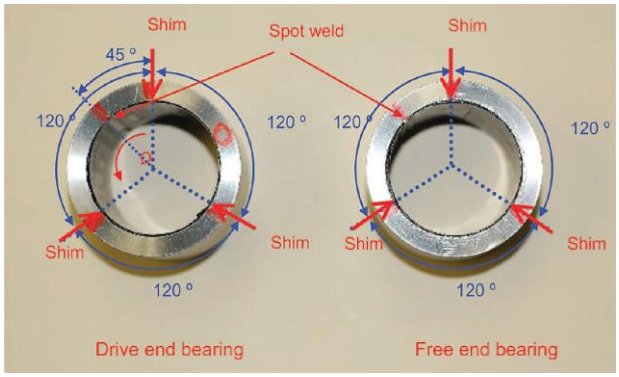

Fig. 2. Metal shims inserted in GFBs [99].

Sim et al. [23] performed rotordynamic analysis and conducted a series of experimental tests for the performance estimation of a turbocharger rotor. The rotor is first driven by compressed air and then by a diesel vehicle engine. The comparative performance of the rotor is investigated by using the original GFB and a modified shimmed GFB which is made up of three additional metal shims under the bump of the GFB. The predictions form the rotordynamic analysis showed that the rotor supported on shimmed GFBs have greater rigid body mode critical speeds than the original GFBs. This is because the shims inserted in the GFBs resulted in considerable increases in direct stiffness coefficients of the shimmed GFB. The experimental investigations depict dominant synchronous motions while using the original as well as modified GFB. However, a significant reduction is observed in the subsynchronous amplitude with the use of shimmed GFB compared to that of the original GFB. Similar rotor behavior is also observed while using the diesel vehicle test bench, implying well agreement with the results of the compressed air test rig [100].

4.2 Active control

Piezoelectric Transducers (PZTs) are intelligent materials that are used for electromechanical coupling. Park et al. [101] arranged a stack of

PZTs both radially and circumferentially in a GFB's bushing. Active control of GFB is achieved by adjusting the clearance and preload through PZT activation. It is found that the film thickness and pressure profile are different due to the PZT activation as compared to without PZT activation. Due to the preload control, however, the film thickness is reduced, and the pressure is increased at preload points. Moreover, the amplitude of vibration in both horizontal and vertical directions is drastically reduced with the control of preload. The integration of PZTs inside the GFB bushing leads to higher stability as the stiffness and journal eccentricity of the bearing are controlled [102]. It is observed that the difference between the direct and cross-coupled stiffness is increased with the increase of activation voltage of the PZTs. This indicates the beneficial effect of the PZTs in stabilizing the performance of the rotor.

4.3 Impact load

Impact load excitations are often employed to study the dynamic response, as these are critical to assess the stability of the rotor-bearing system. Arora et al. [103] performed an impact test to evaluate the stiffness of a GFB that supports a high-speed rotor rotating at 60,000 rpm. It was observed that the stiffness coefficients gradually increase with the rotational speed because of the hardening effect of the gas film. Subsequently, San Andrés et al. [19,20] used the impact load tests to determine the bearing dynamic coefficients of a metal mesh foil bearing. The load tests were conducted with a journal rotating at 50,000 rpm. It was observed that the direct, as well as cross-coupled stiffness values increased with the rising excitation frequency. However, the damping values were found to be decreasing with the rising frequency. The coast down response of the rotor was obtained for both lightly and heavily loaded conditions. Subharmonic whirl motions were observed at system natural frequencies during coast down. At low loads, the bearing exhibits a whirling motion at the half frequency that disappears when the static load is increased.

4.4 Dynamic shaker and load-deflection

An adequate amount of stiffness and damping of the GFB is essential for the stable operation of the GFBR system [104]. The dynamic coefficients are estimated using force sensors and load cells. Electronic actuators are used to provide small amplitude displacements to the GFB at a particular frequency. Then, the restoring force is measured to calculate the stiffness and damping. Salehi et al. [105] used a dynamic shaker to characterize the behavior of a GFB. The dynamic shaker produced the input signal, while separate sensors measured the resulting motion, acceleration, and force. The damping coefficient was found to decrease with the rise in frequency and amplitude, whereas it was increased with the rise in the external load. The stiffness value, however increased with the rise in perturbation frequency. Load-deflection curves and hysteresis loops are also helpful in evaluating the stiffness and damping of the GFB. Rubio et al. [106] performed load-deflection tests on a commercial GFB. The structural stiffness was measured and was found to increase with the rise in the radial deflection of the bump foil. Zhou et al. [107] obtained the hysteresis force–displacement curves for the GFB under quasi-static and dynamic loading and unloading. The hysteresis loops were observed to be flat at higher load-perturbation frequencies, indicating a considerable decrease in energy dissipation. The influence of the friction coefficient on the OSI was also studied. It was found that a minor increase in the friction coefficient results in a significant improvement in the OSI of the GFBR system. Moreover, there is an increase in the stiffness with the increase in friction coefficient, which helps to improve the stability of the system.

4.5 Equivalent viscous damping

Appropriate damping capacity is a major technological barrier to the wide application of GFBs in turbomachinery [108]. Lee et al. [109] proposed the use of viscoelastic foil bearing for turbomachinery to overcome the lack of damping capacity, as shown in Fig. 3. Structural dynamic test was conducted for both viscoelastic foil bearing and GFB. It was observed that the stiffness and damping of the former were much higher than that of the latter. A test setup was designed for the stability study of the rotor bearing system beyond bending critical speed. The first bending critical speed of the rotor was found to be 30,000 rpm, and the rotor was operated up to 50,000 rpm. The vibration amplitude near the first bending

critical speed of the rotor supported on a viscoelastic foil bearing was much lesser than that of the GFB. When operated at 50,000 rpm beyond the first bending critical speed, the GFBR system exhibited nonsynchronous orbits. However, the nonsynchronous orbits were significantly subdued with the use of viscoelastic foil bearings. It is clear that the viscoelastic foil bearing provides sufficient equivalent viscous damping to enable the super bending critical speed operation of the rotor. The bearing is also useful in suppressing the nonsynchronous amplitude of vibrations in rotors.

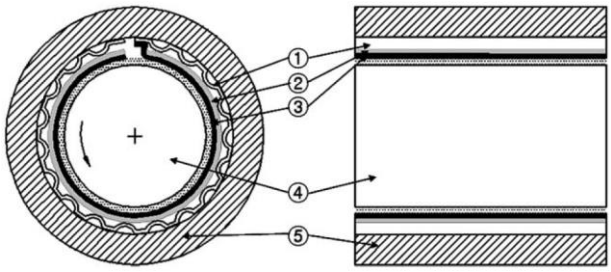

Fig. 3. Structure of a GFB with viscoelastic foil layer: (1) bump foil, (2) viscoelastic foil, (3) top foil, (4) journal, (5) bearing sleeve [109].

Subsequently, the numerical results were predicted using rotordynamic analysis and compared with the previous experimental results [110]. The results agree well when the rotating speed is below the bending critical speed. However, significant errors were found in the results of numerical predictions beyond the first bending critical speed. The numerical analysis was unable to predict the asynchronous motions of the bump foil bearing. The stability of viscoelastic foil bearing and the bump foil bearing supported rotor was further investigated in a two stage centrifugal compressor [111]. The steady aerodynamic response of the bump foil bearing at the compressor end showed that the synchronous motions dominate in the x-direction. The vibration spectrum of the unsteady pressure near the surge line depicted multiple frequencies of subsynchronous motions that correspond to rigid body mode natural frequencies. The spectrum of shaft vibrations with bump foil bearings depicted a smaller amplitude of synchronous motions than that of subsynchronous motions. The vibration spectrum of unsteady pressure at compressor end with viscoelastic foil bearing showed a similar vibration spectrum as that of conventional bump foil bearing. However, it was evident from the spectrum of shaft vibrations that the magnitude of subsynchronous motions was significantly reduced as compared to bump foil bearing. It was clear that subsynchronous motions were effectively controlled by the increased damping capacity in the case of viscoelastic foil bearings.

4.6 Imbalance mass

GFBs must be able to withstand unbalance force, which is one of the essential design parameters for turbomachinery. Sometimes imbalance masses are added to the rotor to induce or balance the nonlinear response and study the coast down motion. Due to the increasing imbalance in the rotor, a forced nonlinearity is induced in the GFB. San Andrés et al. [112] analyzed the performance of the FE model of a test rotor supported on GFB. The amplitudes of response and whirl frequency ratio were recorded for various imbalance loads. Significant synchronous motion is observed for an imbalance displacement of 7.4 μm during the entire speed range. As the imbalance increases to 10.5 μm, subsynchronous vibrations start to appear during the coast down range of 20,500 rpm to 12,500 rpm. The subsynchronous motions are observed at various whirl frequency ratios denoting transient rub action between the rotor and the foil bearing. Also, at lower rotor speed, multiple whirl ratios signify contact with foil during the stoppage of the rotor. Larsen et al. [113] obtained the nonlinear steady state results from the rotordynamic analysis of the GFBR system. A periodic orbit plot is observed at low rotor unbalance, which shows that the synchronous motions are dominant. As the unbalance level is increased, the subsynchronous motions start to appear, which is denoted by a distorted orbit plot. Another important observation is made when the nature of orbits kept changing between distorted and elliptical patterns with the gradual increase of rotor speed. This denotes that the subsynchronous motions emerge and subside with the change of rotor speed and the subsynchronous motion is a function of both rotor unbalance and speed. The sensitivity of the subsynchronous to rotor imbalance was also observed in experimental investigation [114]. It is observed that the amplitude of subsynchronous motions is much bigger than synchronous amplitudes for the

higher imbalance state. Guo et al. [115] studied the influence of static load and unbalanced mass on the GFBR system's nonlinear response using the TM method. As the static load rises, it is observed that subsynchronous motions start to occur, and the speed of measured peak amplitude of synchronous motion goes on increasing. Various coast down tests was conducted with the decreasing imbalance mass. It is found that the subsynchronous motions gradually disappear as the imbalance decreases. Also, the speed of synchronous peak response is almost unchanged at different imbalance conditions. Balducchi et al. [116] obtained the unbalance response of rigid rotor supported on GFBs in x and y directions. It is observed that the amplitude of the response is very small at the starting of the rotor, implying rubbing between the foil and the rotor. As the unbalance increases, there is a nonlinear rise in the amplitude response of the bearing. Similar characteristics are obtained for a turbocharger rotor supported on GFB, where the response is fairly small when the rotor is riding on the compliant foil [117]. After that, the response increases and remains steady, indicating the shaft has become airborne. Bonello and Hassan [118] numerically and experimentally tested a GFBR system performance. The waterfall plots are obtained with added unbalance. It was observed that the subsynchronous frequency trains appear with the increase of unbalance. The OSI was found to be decreased with the increase of unbalance mass. The measured orbits were considerably larger than the predicted ones due to the influence of residual unbalance. Similar observations were made with a gas foil bearing test rig [119]. The results denoted enhanced subharmonic motions of multiple orders with the increased unbalance mass. It is observed that there is a considerable reduction in the local stiffness of the bump foil with the increased unbalance. This results in a decrease in the OSS motion, which denotes the destabilizing effects of increasing unbalance mass.

4.7 Thermal management

In GFBs, there is no requirement of pressurized gas as the hydrodynamic pressure is generated due to the fluid film, rotating action between the rotor and top foil. However, pressurized cooling gas flow is often introduced in GFBs for thermal management. It is one of the most prevalent methods of heat removal, which prevents the GFBs from thermal seizure [120]. This helps in removing heat from drag or reducing thermal gradients between hot and cool engine components. Radil et al. [121] presented three distinct approaches of leveraging air to offer thermal management in GFBR systems. The first one is by direct deposition of air on the inner surface of the journal, as shown in Fig. 4. The second approach is by an indirect axial flow of air through the test journal, as shown in Fig. 5. The last one is by a forced axial flow of air through the support structure of the bearing, as shown in Fig. 6. The experiments show that all three approaches provide heat control at varying degrees of efficacy.

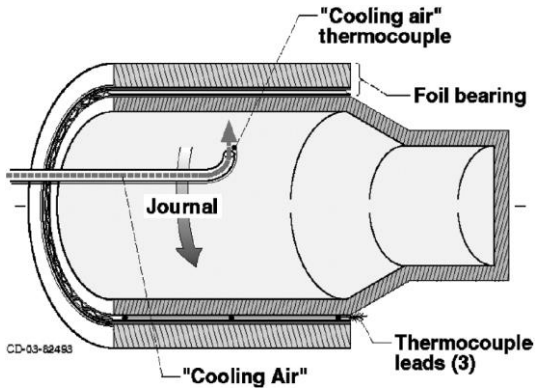

Fig. 4. Direct cooling method [121].

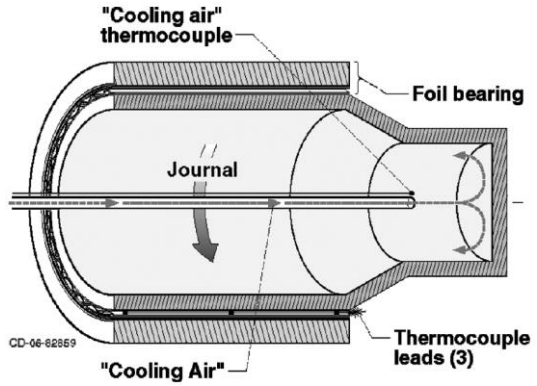

Fig. 5. Indirect cooling method [121].

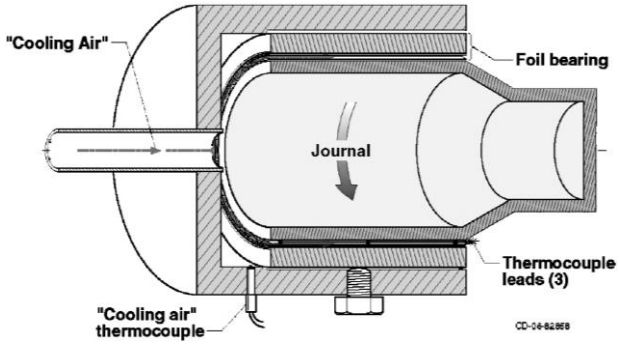

Fig. 6. Forced axial cooling method [121].

Heshmat et al. [122] tested a turbojet engine rotor with an appropriate supply of cooling flow into the GFB. Successful endurance tests were conducted up to a speed of 120,000 rpm at an operating temperature of 800°C. Kim et al. [123] analysed the effect of gas flow during run up operation of a GFBR system. Run up test was conducted up to 35,000 rpm with increasing feed pressure to 2.8 bars. It is observed that there is a delay in the OSS motions with the increase of feed pressure. Moreover, the subsynchronous motions gradually start to disappear as the side pressure rises in the GFB denoting stable response of the rotor. San Andrés et al. [124,125] investigated the run up and coastdown operation of a GFBR system under hot conditions. The heat was supplied by an electric cartridge heater. When no heat was supplied to the shaft, the rotor amplitude was found to drop abruptly just above the critical speed. This suggests that there is a forced nonlinearity in the GFB, which is one of the major causes of subsynchronous motions in GFBs. When the temperature of the rotor is increased, the amplitude of motion gradually decreases, and no abrupt jump is visible. The coast down response reveals that the system's critical speed increases moderately with the increase of temperature, and there is a considerable drop in the peak amplitude of motion. Moreover, during coast down, an exponential decay in the rotor speed was observed with respect to time. This suggests the availability of viscous drag during operation in a hot environment. So the cooling flow is often used as a solution to remove heat from the viscous drag. It was also observed that in spite of supplying high flow of cooling gas, the overall bearing temperature was dropped by just few degrees [126]. Waterfall plots are obtained at room temperature, which showed dominating synchronous rotor motions with minor subsynchronous motions. As the temperature of the system is increases, there is a decrease in the peak amplitude of synchronous motions. However, there is a moderate increase in the critical speed with the rise of temperature from the ambient conditions. Recently, smart materials and thermoelectric modules (TEMs) have been extensively used to control thermal conditions. Feng et al. [24] used the shape memory alloy (SMA) wires in the place of bump foils of a GFB. The objective was to control the active elasto-damping properties by means of thermal activation. Electric current was supplied, and axially installed pipes were used to heat and cool the SMA wires. The response time for phase transformation of the SMA wires was noted. It was observed that the SMA wires martensite to austenite transformation took 2 seconds whereas 4 seconds for the vice versa when cooled. This depicts the ability of the SMA-GFB to swiftly adapt to changing operating conditions. Later, this effect of non-isothermal phase transformations was included in the model of an SMA-based GFB [127,128]. It was depicted that the thermal and mechanical response of the SMA wires can be modeled which is helpful in developing solid-state actuators and dampers. TEMs and TCs can be utilized to manage heat flow and dissipation in GFBs [129]. TEMs are composed of semiconductors that enable heat energy passage, whereas TCs monitor temperatures at specified locations in GFBs. Baginski et al. [130] suggested an active cooling technique using TEMs mounted in the bushing of the GFB. The temperature of the outer surface of the top foil was measured using TCs. It was observed that the average temperature of the bearing was significantly reduced without compromising the dynamic characteristics of the shaft's journal. Thermal management in GFBs can also be achieved by controlling the temperature gradients [131]. A prototype model was built with 36 TEMs installed in the GFB. A simple adaptive algorithm was used to control the thermal characteristics of the foil. The control technique enabled a considerable decrease in the temperature gradient.

5. DISCUSSIONS AND FUTURE PROSPECTS

Some areas in the field of rotordynamic systems supported on gas foil bearings, which may be taken up in a greater situation, are the following.

1. Dynamic coefficients are vital to access the dynamic characteristics of the GFBs. Stiffness and damping are dependent on the combined impacts of the gas film's hydrodynamics and the structural dynamics of the supporting foil. However, the majority of the research is focused on tailoring the structural dynamics as its stiffness is comparatively much lower than the gas film's stiffness during the operations.

2. Lower friction coefficients result in softer bumps with more deflection in both vertical and horizontal directions. Also, an increase in the friction coefficients at the contacts results in Coulomb damping and increased stiffness. Researchers have suggested various models that incorporate friction in GFB. However, the use of solid lubricants in GFBs has not yet been explored, as they can be an excellent additive to reduce friction.
3. In the numerous numerical analyses that are utilized nowadays, it is still required to improve the accuracy of the models, especially given the high-speed applications these bearings are being used. While several of the models agreed rather well with the experimental data, the models need to be made adaptable to capture all of the behaviors in a high-speed environment.
4. The critical fluid and structural aspects of GFBs were captured by the finite element, finite difference, or control volume methods described in the studies. Combining these methods to capture more phenomena in a single model might improve the accuracy. However, combining the models might result in high processing durations.
5. In order to improve the accuracy of the structural aspect of GFB modeling, various factors must be taken into account, such as bump interaction, friction forces between bump foil and top foil, and bump foil and bearing base and elasticity of bump foil. Furthermore, in order to properly compute the deflection of the top foil, the lateral deflection of the flat section between two subsequent bumps must be considered.
6. GFBs are susceptible to subsynchronous motions such as the whirl and whip frequencies. Researchers have suggested that the nature of the gas film and the foil structure deformations affect the stiffness of the GFB, which in turn governs the subsynchronous motions. However, the possible ways to adjust the whirl and whip frequencies by tailoring the stiffness of the bump is an aspect that still remains to be investigated.
7. The speed of initiation of subsynchronous motions goes on increasing with the increasing mechanical preload. However, highly preloaded bearings are susceptible to thermal runaway. Therefore, it is important to determine the optimum preload for the GFBs.
8. The amplitude of vibration and nonsynchronous orbits are subdued by the use of a viscoelastic foil bearing. Therefore, researchers should take more interest in tailoring the equivalent viscous damping of GFBs.
9. GFBs are often coated to improve their thermal properties. However, the effect of coated rotors and foils on the stability of the GFBR system still remains to be investigated.
10. As the unbalance increases, there is a nonlinear rise in the response amplitude of the GFB. Unbalance control has received much attention in the magnetic bearing rotor system. However, this unbalance control aspect can be implemented in foil bearings by using a hybrid foil magnetic bearing.
11. For the studies on dynamic aspects of the GFBR systems, the research is mainly focused on the motion studies of the rotor. Minor importance is given to GFB design parameters which induce strong nonlinear characteristics in rotors. The methods to tailor these design parameters in order to contain the instability in GFBR systems still remain an active area of investigation.

6. CONCLUSION

The work presented in this review is a humble attempt to understand the current progress on various methodologies used for performance prediction of GFB and its implementation to high-speed rotors. GFBs show very complicated behavior compared to other bearings. Various analytical models utilized to simulate the GFB performance are discussed, as well as their predictions and correlations with experimental data. The study of static and dynamic characterization, as well as relevant issues encountered during the GFB analysis, are presented. The research efforts to gain insight into the strong influence of GFB parameters on the nonlinear behavior of various turbomachinery are addressed. The nonlinearity in GFBs, their impact on the instability as well as the major causes of subsynchronous motions are discussed. The countermeasures that are relevant to mitigate the instability are presented.

This review aims to provide a systematic and comprehensive analysis of the latest research progress on the performance prediction of GFB as well as its stability in high-speed operation. For the convenience of the researchers, the key points of the review are presented as follows.

1. The increase in the compliance of the GFB results in decreased load-carrying capacity and increased film thickness. Therefore, at low loads, it is preferable to use high-compliance bearings.
2. The stiffness coefficients are found to rise as the bearing number rises and decline as the bearing compliance rises. The damping coefficients, however, progressively grow with the bearing number, reach a maximum, and then decline.
3. Bump interaction must be considered in the structural model; otherwise, the bump flexibility is overestimated.
4. An increase in the friction coefficients at the contact surface results in Coulomb damping and increased stiffness.
5. The inclusion of the slip-flow effect in the GFB model resulted in decreased load-carrying capacity and increased attitude angle.
6. FD method is often used for GFB models as it can solve higher-order schemes. However, it cannot accumulate non-regular solutions and is only feasible for structured models.
7. Although the CV method is straightforward and commands less computational effort, it is not often used for GFB modeling because of the difficulty in solving higher-order schemes.
8. FE method is that it can be used to model any complex shaped geometry using the element formulation of the Reynolds equation. However, the FE method requires more mathematics than any other method, which might increase the computational time.
9. Linear frequency domain simulation is not sufficient for the stability analysis of the GFBs. Nonlinear TM simulations are required for complete information on the bearing stability.
10. TM method was found to be more accurate than the perturbation method for the stability analysis of the GFB.
11. The speed of initiation of subsynchronous motions goes on increasing with the increasing mechanical preload of the GFB.
12. The integration of PZTs inside the GFB bushing enables the control of stiffness and journal eccentricity, which leads to higher stability.
13. Sufficient equivalent viscous damping in GFBs enables to subdue the subsynchronous motions in GFBR systems.
14. The subsynchronous motion in the GFBR system is a function of both rotor unbalance and speed.
15. The supply of electric current enables the phase transformation and heating of the SMA wires, which in turn controls the active elasto-damping properties of the GFB.
16. The active cooling technique using TEMs can significantly reduce the average temperature of the GFB.

Acknowledgement

I gratefully acknowledge all the researchers who have worked in the field of tribology, without their significant contribution. This review literature would have been difficult to summarise.

REFERENCES

[1] K. Czolczynski, *Rotordynamics of gas-lubricated journal bearing systems*, New York: Springer, 1999.

[2] G.L. Agrawal, *Foil Air/Gas Bearing Technology — an overview*, Turbo Expo: Power for Land, Sea and Air, vol. 1, 1997, pp. 1-11, doi: 10.1115/97-gt-347

[3] C. McAuliffe, P.J. Dziorny, *Bearing cooling arrangement for air cycle machine*, United States patent , US5113670A, 1992.

[4] H.M. Chen, R. Howarth, B. Geren, J.C. Theilacker, W.M. Soyars, *Application of Foil Bearings to Helium Turbocompressor*, in Proceedings of the 30th Turbomachinery Symposium, January, 2001, Texas A&M University, Turbomachinery Laboratories, pp. 103-113, doi: 0.21423/R1P06R

[5] E.E. Swanson, H. Heshmat, J.S. Shin, *The role of high performance foil bearings in an advanced, oil-free, integral permanent magnet motor driven, high-speed turbo-compressor operating above the first bending critical speed*, Turbo Expo: Power for Land, Sea and Air, vol. 1, pp. 1119-1125, 2002, doi: 10.1115/gt2002-30579

[6] H. Heshmat, J.F. Walton, A. Hunsberger, *Oil free 8 kw high-speed and high specific power turbogenerator*, Turbo Expo: Power for Land, Sea and Air, vol. 1b, 2014, pp. 1-16, doi: 10.1115/gt2014-27306

[7] Y.M. Yang, B.S. Park, S.W. Lee, D.H. Lee, *Development of a turbo-generator for orc system with twin radial turbines and gas foil bearings*, in Proceedings of the 3rd International Seminar on ORC Power Systems, 12 October, 2015, Brussels, Belgium, pp. 12-14.

[8] H. Heshmat, J.F. Walton, C.D. Corte, M. Valco, *Oil-free turbocharger demonstration paves way to gas turbine engine applications*, Turbo Expo: Power for Land, Sea and Air, vol. 1, 2000, pp. 1-8, doi: 10.1115/2000-gt-0620

[9] K. Ryu, *Oil-free turbocharger bearing assembly having conical shaft supported on compliant gas bearings*, United States patent, US9394941B2, 2016.

[10] M. Salehi, H. Heshmat, J.F. Walton, M. Tomaszewski, *Operation of a mesoscopic gas turbine simulator at speeds in excess of 700,000 rpm on foil bearings*, Journal of Engineering for Gas Turbines and Power, vol. 129, iss. 1, pp. 170–176, 2007, doi: 10.1115/1.2360600

[11] F.J. Suriano, R.D. Dayton, F.G. Woessner, *Test experience with turbine-end foil bearing equipped gas turbine engines*, Turbo Expo: Power for Land, Sea and Air, vol. 2, 1983, pp. 1-6, doi: 10.1115/83-gt-73

[12] Y. Hou, Z.H. Zhu, C.Z. Chen, *Comparative test on two kinds of new compliant foil bearing for small cryogenic turbo-expander*, Cryogenics, vol. 44, iss. 1, pp. 69–72, 2004, doi: 10.1016/j.cryogenics.2003.08.002

[13] L.Y. Xiong, G. Wu, Y. Hou, L.Q. Liu, M.F. Ling, C.Z. Chen, *Development of aerodynamic foil journal bearings for a high speed cryogenic turboexpander*, Cryogenics, vol. 37, iss. 3, pp. 221–230, 1997, doi: 10.1016/S0011-2275(97)00012-X

[14] J.M. Vance, F.Y. Zeidan, B.G. Murphy, *Machinery vibration and rotordynamics*, Wiley, 2010.

[15] K. Shalash, J. Schiffmann, *On the manufacturing of compliant foil bearings*, Journal of Manufacturing Processes, vol. 25, pp. 357–368, 2017, doi: 10.1016/j.jmapro.2016.12.021

[16] D. Kim, *Parametric studies on static and dynamic performance of air foil bearings with different top foil geometries and bump stiffness distributions*, Journal of Tribology, vol. 129, iss. 2, pp. 354–364, 2006, doi: 10.1115/1.2540065

[17] J.H. Song, D. Kim, *Foil gas bearing with Compression Springs: Analyses and experiments*, Journal of Tribology, vol. 129, iss. 3, pp. 628–639, 2007, doi: 10.1115/1.2736455

[18] H.Q. Guan, K. Feng, K. Yu, Y.L. Cao, Y.H. Wu, *Nonlinear dynamic responses of a rigid rotor supported by active bump-type foil bearings*, Nonlinear Dynamics, vol. 100, pp. 2241–2264, 2020, doi: 10.1007/s11071-020-05608-4

[19] L. San Andrés, T.A. Chirathadam, *Identification of rotordynamic force coefficients of a metal mesh foil bearing using impact load excitations*, Journal of Engineering for Gas Turbines and Power, vol. 133, iss. 11, 2011, doi: 10.1115/1.4002658

[20] L. San Andrés, T.A. Chirathadam, *Metal mesh foil bearing: Effect of motion amplitude, rotor speed, static load, and excitation frequency on force coefficients*, Journal of Engineering for Gas Turbines and Power, vol. 133, iss. 12, 2011, doi: 10.1115/1.4004112

[21] K. Sim, Y.B. Lee, T.H. Kim, *Effects of mechanical preload and bearing clearance on Rotordynamic performance of lobed gas foil bearings for oil-free turbochargers*, Tribology Transactions, vol. 56, iss. 2, pp. 224–235, 2013, doi: 10.1080/10402004.2012.737502

[22] K. Sim, Y.B. Lee, T.H. Kim, *Rotordynamic analysis of an oil-free turbocharger supported on lobed gas foil bearings—predictions versus test data*, Tribology Transactions, vol. 57, iss. 6, pp. 1086–1095, 2014, doi: 10.1080/10402004.2014.937885

[23] K. Sim, L. Yong-Bok, T.H. Kim, J. Lee, *Rotordynamic performance of shimmed gas foil bearings for oil-free turbochargers*, Journal of Tribology, vol. 134, iss. 3, 2012, pp. 1-11, doi: 10.1115/1.4005892

[24] K. Feng, Y. Cao, K. Yu, H. Guan, Y. Wu, Z. Guo, *Characterization of a controllable stiffness foil bearing with shape memory alloy springs*, Tribology International, vol. 136, pp. 360–371, 2019, doi: 10.1016/j.triboint.2019.03.068

[25] M. Branagan, D. Griffin, C. Goyne, A. Untaroiu, *Compliant gas foil bearings and Analysis Tools*, Journal of Engineering for Gas Turbines and Power, vol. 138, iss. 5, pp. 1-8, 2015, doi: 10.1115/1.4031628

[26] P. Samanta, N.C. Murmu, M.M. Khonsari, *The evolution of foil bearing technology*, Tribology International, vol. 135, pp. 305–323, 2019, doi: 10.1016/j.triboint.2019.03.021

[27] C. DellaCorte, R.J. Bruckner, *Remaining technical challenges and future plans for oil-free turbomachinery*, Journal of Engineering for Gas Turbines and Power, vol. 133, iss. 4, 2010, doi: 10.1115/1.4002271

[28] C. DellaCorte, M.J. Valco, *Oil-free turbomachinery technology for regional jet, rotorcraft and supersonic business jet propulsion engines*, in Proceedings of the 2003 International Society of Airbreathing Engines Conference, September 2003, Cleveland, Ohio, pp. 2003-1182.

[29] C. DellaCorte, A.R. Zaldana, K.C. Radil, *A systems approach to the solid lubrication of foil air bearings for oil-free turbomachinery*, Journal of Tribology, vol. 126, iss. 1, pp. 200-207, 2004, doi: 10.1115/1.1609485

[30] C. DellaCorte, *Oil-free shaft support system rotordynamics: Past, present and future challenges and opportunities*, Mechanical Systems and Signal Processing, vol. 29, pp. 67-76, 2012, doi: 10.1016/j.ymssp.2011.07.024

[31] D. Dowson, *A generalized Reynolds equation for fluid-film lubrication*, International Journal of Mechanical Sciences, vol. 4, iss. 2, pp. 159–170, 1962, doi: 10.1016/s0020-7403(62)80038-1

[32] H. Heshmat, J.A. Walowit, O. Pinkus, *Analysis of gas-lubricated foil journal bearings*, Journal of Lubrication Technology, vol. 105, iss. 4, pp. 647–655, 1983, doi: 10.1115/1.3254697

[33] J.A. Walowit, J.N. Anno, B.J. Hamrock, *Modern developments in lubrication mechanics*, Journal of Lubrication Technology, vol. 99, iss. 2, pp. 304–305, 1977, doi: 10.1115/1.3453088

[34] H. Heshmat, J.A. Walowit, O. Pinkus, *Analysis of gas lubricated compliant thrust bearings*, Journal of Lubrication Technology, vol. 105, iss. 4, pp. 638–646, 1983, doi: 10.1115/1.3254696

[35] J.P. Peng, M. Carpino, *Calculation of stiffness and damping coefficients for elastically supported gas foil bearings*, Journal of Tribology, vol. 115, iss. 1, pp. 20–27, 1993, doi: 10.1115/1.2920982

[36] H. Bensouilah, M. Lahmar, B. Bou-Saïd, *Elasto-aerodynamic lubrication analysis of a self-acting air foil journal bearing*, Lubrication Science, vol. 24, iss. 3, pp. 95–128, 2012, doi: 10.1002/ls.171

[37] T.H. Kim, L. San Andrés, *Heavily loaded gas foil bearings: A model anchored to test data*, Journal of Engineering for Gas Turbines and Power, vol. 130, iss. 1, pp. 1-8, 2008, doi: 10.1115/1.2770494

[38] N.S. Lee, D.H. Choi, Y.B. Lee, T.H. Kim, C.H. Kim, *The influence of the slip flow on steady-state load capacity, stiffness and damping coefficients of elastically supported gas foil bearings*, Tribology Transactions, vol. 45, iss. 4 pp. 478–484, 2002, doi: 10.1080/10402000208982577

[39] Z.C. Peng, M.M. Khonsari, *Hydrodynamic analysis of compliant foil bearings with Compressible Air Flow*, Journal of Tribology, vol. 126, iss. 3, pp. 542–546, 2004, doi: 10.1115/1.1739242

[40] I. Iordanoff, *Analysis of an aerodynamic compliant foil thrust bearing: Method for a rapid design*, Journal of Tribology, vol. 121, iss. 4, pp. 816–822, 1991, doi: 10.1115/1.2834140

[41] J.P. Peng, M. Carpino, *Coulomb friction damping effects in elastically supported gas foil bearings©*, Tribology Transactions, vol. 37, no. 1, pp. 91–98, 1994, doi: 10.1080/10402009408983270

[42] J.S. Larsen, I.F. Santos, *Efficient solution of the non-linear Reynolds equation for compressible fluid using the finite element method*, Journal of the Brazilian Society of Mechanical Sciences and Engineering, vol. 37, iss. 3, pp. 945–957, 2014, doi: 10.1007/s40430-014-0220-5

[43] J.S. Larsen, A.C. Varela, I.F. Santos, *Numerical and experimental investigation of bump foil mechanical behaviour*, Tribology International, vol. 74, pp. 46–56, 2014, doi: 10.1016/j.triboint.2014.02.004

[44] C.P.R. Ku, H. Heshmat, *Compliant foil bearing structural stiffness analysis: Part I—theoretical model including strip and variable bump foil geometry*, Journal of Tribology, vol. 114, iss. 2, pp. 394–400, 1992, doi: 10.1115/1.2920898

[45] C.P.R. Ku, H. Heshmat, *Compliant foil bearing structural stiffness analysis—PART II: Experimental investigation*, Journal of Tribology, vol. 115, iss. 3, pp. 364–369, 1993, doi: 10.1115/1.2921644

[46] C.P.R. Ku, H. Heshmat, *Structural stiffness and coulomb damping in compliant foil journal Bearings: Parametric Studies*, Tribology Transactions, vol. 37, iss. 3, pp. 455–462, 1994, doi: 10.1080/10402009408983317

[47] C.P.R. Ku, H. Heshmat, *Structural stiffness and coulomb damping in compliant foil journal Bearings: Theoretical considerations*, Tribology Transactions, vol. 37, iss. 3, pp. 525–533, 1994, doi: 10.1080/10402009408983325

[48] C.P.R. Ku, H. Heshmat, *Effects of static load on dynamic structural properties in a flexible supported foil journal bearing*, Journal of Vibration and Acoustics, vol. 116, iss. 3, pp. 257–262, 1994, doi: 10.1115/1.2930422

[49] J.P. Peng, M. Carpino, *Finite element approach to the prediction of foil bearing rotor dynamic coefficients*, Journal of Tribology, vol. 119, iss. 1, pp. 85–90, 1997, doi: 10.1115/1.2832484

[50] D.H. Lee, Y.C. Kim, K.W. Kim, *The Dynamic Performance Analysis of foil journal bearings considering coulomb friction: Rotating unbalance response*, Tribology Transactions, vol. 52, iss. 2, pp. 146–156, 2009, doi: 10.1080/10402000802192685

[51] K. Feng, Z. Guo, *Prediction of dynamic characteristics of a bump-type foil bearing structure with consideration of dynamic friction*, Tribology Transactions, vol. 57, iss. 2, pp. 230–241, 2014, doi: 10.1080/10402004.2013.864790

[52] D.H. Lee, Y.C. Kim, K.W. Kim, *The effect of coulomb friction on the static performance of Foil Journal Bearings*, Tribology International, vol. 43, iss. 5-6, pp. 1065–1072, 2010, doi: 10.1016/j.triboint.2009.12.048

[53] A. Fatu, M. Arghir, *Numerical Analysis of the impact of manufacturing errors on the structural stiffness of foil bearings*, Journal of Engineering for Gas Turbines and Power, vol. 140, iss. 4, pp. 1-9, 2017, doi: 10.1115/1.4038042

[54] M. Arghir, O. Benchekroun, *A simplified structural model of bump-type foil bearings based on contact mechanics including gaps and friction*, Tribology International, vol. 134, pp. 129–144, 2019, doi: 10.1016/j.triboint.2019.01.038

[55] P. Hryniewicz, M. Wodtke, A. Olszewski, R. Rzadkowski, *Structural properties of foil bearings: A closed-form solution validated with finite element analysis*, Tribology Transactions, vol. 52, iss. 4, pp. 435–446, 2009, doi: 10.1080/10402000802687916

[56] K. Feng, S. Kaneko, *Analytical model of bump-type foil bearings using a link-spring structure and a finite-element shell model*, Journal of Tribology, vol. 132, iss. 2, pp. 1-11, 2010, doi: 10.1115/1.4001169

[57] S. Le Lez, M. Arghir, J. Frene, *Static and dynamic characterization of a bump-type foil bearing structure*, Journal of Tribology, vol. 129, iss. 1, pp. 75–83, 2006, doi: 10.1115/1.2390717

[58] S. Le Lez, M. Arghir, J. Frene, *A new bump-type foil bearing structure analytical model*, Journal of Engineering for Gas Turbines and Power, vol. 129, iss. 4, pp. 1047–1057, 2007, doi: 10.1115/1.2747638

[59] A.M. Gad, S. Kaneko, *A new structural stiffness model for bump-type foil bearings: Application to generation II gas lubricated foil thrust bearing*, Journal of Tribology, vol. 136, iss. 4, pp. 1-13, 2014, doi: 10.1115/1.4027601

[60] A.M. Gad, S. Kaneko, *Performance characteristics of gas-lubricated bump-type foil thrust bearing*, Proceedings of the Institution of Mechanical Engineers, Part J: Journal of Engineering Tribology, vol. 229, iss. 6, pp. 746–762, 2014, doi: 10.1177/1350650114564709

[61] A.M. Gad, S. Kaneko, *Tailoring of the bearing stiffness to enhance the performance of gas-lubricated bump-type foil thrust bearing*, Proceedings of the Institution of Mechanical Engineers, Part J: Journal of Engineering Tribology, vol. 230, iss. 5, pp. 541–560, 2015, doi: 10.1177/1350650115606482

[62] M. Carpino, J.P. Peng, *Theoretical performance of foil journal bearings*, in 27th Joint propulsion conference, 24-26 June, Sacramento, USA, 1991, doi: 10.2514/6.1991-2105

[63] M. Carpino, G. Talmage, *A fully coupled finite element formulation for elastically supported foil journal bearings*, Tribology Transactions, vol. 46, iss. 4, pp. 560–565, 2003, doi: 10.1080/10402000308982664

[64] M. Carpino, G. Talmage, *Prediction of rotor dynamic coefficients in gas lubricated foil journal bearings with corrugated sub-foils*, Tribology Transactions, vol. 49, iss. 3, pp. 400–409, 2006, doi: 10.1080/10402000600781416

[65] M. Carpino, L.A. Medvetz, J.P. Peng, *Effects of membrane stresses in the prediction of foil Bearing performance©*, Tribology Transactions vol. 37, iss. 1, pp. 43–50, 1994, doi: 10.1080/10402009408983264

[66] M. Carpino, J.P. Peng, L. Medvetz, *Misalignment in a complete Shell gas foil journal bearing*, Tribology Transactions, vol. 37, iss. 4, pp. 829–835, 1994, doi: 10.1080/10402009408983365

[67] S. von Osmanski, J.S. Larsen, I.F. Santos, *A fully coupled air foil bearing model considering friction – theory & experiment*, Journal of Sound and Vibration, vol. 400, pp. 660–679, 2017, doi: 10.1016/j.jsv.2017.04.008

[68] S.P. Bhore, A.K. Darpe, *Nonlinear transient stability analysis of meso-scale rotor supported on gas foil journal bearings*, Journal of Vibration Engineering & Technologies, vol. 7, iss. 4, pp. 399–406, 2019, doi: 10.1007/s42417-019-00128-x

[69] S.P. Bhore, A.K. Darpe, *Nonlinear Dynamics of flexible rotor supported on the gas foil journal bearings*, Journal of Sound and Vibration, vol. 332, iss. 20, pp. 5135–5150, 2013, doi: 10.1016/j.jsv.2013.04.023

[70] M.A. Shahdhaar, S.S. Yadawad, D.S. Khamari, S.K. Behera, *Numerical investigation of slip flow phenomenon on performance characteristics of gas foil journal bearing*, SN Applied Sciences, vol. 2, iss. 10, pp. 1-8, 2020, doi: 10.1007/s42452-020-03494-4

[71] J. Kumar, D.S. Khamari, S.K. Behera, R.K. Sahoo, *Investigation of thermohydrodynamic behaviour of gas foil journal bearing accounting slip-flow phenomenon*, Journal of the Brazilian Society of Mechanical Sciences and Engineering, vol. 44, iss. 1, pp. 1-19, 2021, doi: 10.1007/s40430-021-03330-9

[72] J. Kumar, D.S. Khamari, S.K. Behera, R.K. Sahoo, *Influence of slip-flow phenomenon on thermohydrodynamic behaviour of gas foil thrust bearings*, Proceedings of the Institution of Mechanical Engineers, Part J: Journal of Engineering Tribology, vol. 236, iss. 1, pp. 15–30, 2021, doi: 10.1177/13506501211002962

[73] D.S. Khamari, J. Kumar, S.K. Behera, *Numerical investigation of influence sensitivity of a gas foil bearing parameters on the dynamic coefficients*, Journal of the Brazilian Society of Mechanical Sciences and Engineering, vol. 43, iss. 3, pp. 1-9, 2021, doi: 10.1007/s40430-021-02874-0

[74] J. Kumar, D.S. Khamari, S.K. Behera, R.K. Sahoo, *A methodology for performance prediction: Aerodynamic analysis of axially loaded gas foil bearing*, Sādhanā, vol. 46, iss. 4, pp. 1-20, 2021, doi: 10.1007/s12046-021-01721-1

[75] K. Feng, S. Kaneko, *A numerical calculation model of multi wound foil bearing with the effect of foil local deformation*, Journal of System Design and Dynamics, vol. 1, iss. 3, pp. 648–659, 2007, doi: 10.1299/jsdd.1.648

[76] Y.B. Lee, D.J. Park, C.H. Kim, S.J. Kim, *Operating characteristics of the bump foil journal bearings with top foil bending phenomenon and correlation among bump foils*, Tribology International, vol. 41, iss. 4, pp. 221–233, 2008, doi: 10.1016/j.triboint.2007.07.003

[77] L. San Andre´s, T.H. Kim, *Improvements to the analysis of gas foil bearings: Integration of top foil 1D and 2d structural models*, Turbo Expo: Power for Land, Sea, and Air, vol. 5, 2007, pp. 1-11, doi: 10.1115/gt2007-27249

[78] L. San Andrés, T.H. Kim, *Analysis of gas foil bearings integrating FE Top Foil Models*, Tribology International, vol. 4, iss. 1, pp. 111–120, 2009, doi: 10.1016/j.triboint.2008.05.003

[79] D. Ruscitto, J. McCormick, S. Gray, *Hydrodynamic air lubricated compliant surface bearing for an automotive gas turbine engine. I. Journal Bearing Performance*, Technical Report, 1978, doi: 10.2172/7095892

[80] D.H. Lee, Y.C. Kim, K.W. Kim, *The Static Performance Analysis of foil journal bearings considering three-dimensional shape of the foil structure*, Journal of Tribology, vol. 130, iss. 3, 2008, pp. 1-10, doi: 10.1115/1.2913538

[81] F. Xu, Z. Liu, G. Zhang, L. Xie, *Hydrodynamic analysis of compliant foil bearings with modified top foil model*, Structures and Dynamics, Parts A and B, vol. 6, pp. 1-10, 2011, doi: 10.1115/gt2011-46018

[82] F. Xu, Z. Liu, G. Zhang, Z. Cao, *Effects of shear stiffness in top foil structure on gas foil bearing performance based on thick plate theory*, Proceedings of the Institution of Mechanical Engineers, Part J: Journal of Engineering Tribology, vol. 227, iss. 7, pp. 761–776, 2012, doi: 10.1177/1350650112468071

[83] B.B. Nielsen, I.F. Santos, *Transient and Steady State Behaviour of elasto–aerodynamic air foil bearings, considering bump foil compliance and top foil inertia and flexibility: A numerical investigation*, Proceedings of the Institution of Mechanical Engineers, Part J: Journal of Engineering Tribology, vol. 231, iss. 10, pp. 1235-1253, 2017, doi: 10.1177/1350650117689985

[84] H. Heshmat, W. Shapiro, S. Gray, *Development of foil journal bearings for high load capacity and high speed whirl stability*, Journal of Lubrication Technology, vol. 104, iss. 2, pp. 149–156, 1982, doi: 10.1115/1.3253173

[85] H. Heshmat, *Advancements in the performance of aerodynamic foil journal bearings: High Speed and load capability*, Journal of Tribology, vol. 116, iss. 2, pp. 287–294, 1994, doi: 10.1115/1.2927211

[86] H. Heshmat, *Operation of foil bearings beyond the bending critical mode*, Journal of Tribology. Vol. 122, iss. 1, pp. 192–198, 1999, doi: 10.1115/1.555342

[87] J.S. Larsen, I.F. Santos, S. von Osmanski, *Stability of rigid rotors supported by air foil bearings: Comparison of two fundamental approaches*, Journal of Sound and Vibration, vol. 381, pp. 179–191, 2016, doi: 10.1016/j.jsv.2016.06.022

[88] S. von Osmanski, J.S. Larsen, I.F. Santos, *Multi-domain stability and modal analysis applied to gas foil bearings: Three approaches*, Journal of Sound and Vibration, vol. 472, 2020, doi: 10.1016/j.jsv.2020.115174

[89] Q. Zhou, Y. Hou, C. Chen, *Dynamic stability experiments of compliant foil thrust bearing with viscoelastic support*, Tribology International, vol. 42, iss. 5, pp. 662–665, 2009, doi: 10.1016/j.triboint.2008.09.005

[90] T.H. Kim, Y.-B. Lee, T.Y. Kim, K.H. Jeong, *Rotordynamic performance of an oil-free turbo blower focusing on load capacity of gas foil thrust bearings*, Journal of Engineering for Gas Turbines and Power, vol. 134, iss. 2, 2011, doi: 10.1115/1.4004143

[91] G. Grau, I. Iordanoff, B. Bou Said, Y. Berthier, *An original definition of the profile of compliant foil journal gas bearings: Static and dynamic analysis*, Tribology Transactions, vol. 47, iss. 2, pp. 248–256, 2004, doi: 10.1080/05698190490439157

[92] J.F. Walton, H. Hesmat, *Application of foil bearings to turbomachinery including vertical operation*, Journal of Engineering for Gas Turbines and Power, vol. 124, iss. 4, pp. 1032–1041, 2002, doi: 10.1115/1.1392986

[93] J.F. Walton, H. Heshmat, M.J. Tomaszewski, *Testing of a small turbocharger/turbojet sized simulator rotor supported on foil bearings*, Turbo Expo: Power for Land, Sea, vol. 6, 2004, pp. 1-7, doi: 10.1115/gt2004-53647

[94] Z. Guo, K. Feng, T. Liu, P. Lyu, T. Zhang, *Nonlinear dynamic analysis of rigid rotor supported by gas foil bearings: Effects of gas film and foil structure on subsynchronous vibrations*, Mechanical Systems and Signal Processing, vol. 107, pp. 549–566, 2018, doi: 10.1016/j.ymssp.2018.02.005

[95] Z. Guo, L. Peng, K. Feng, W. Liu, *Measurement and prediction of nonlinear dynamics of a gas foil bearing supported rigid rotor system*, Measurement, vol. 121, pp. 205–217, 2018, doi: 10.1016/j.measurement.2017.12.039

[96] H.Q. Guan, K. Feng, Y.L. Cao, M. Huang, Y.H. Wu, Z.Y. Guo, *Experimental and theoretical investigation of rotordynamic characteristics of a rigid rotor supported by an active bump-type foil bearing*, Journal of Sound and Vibration, vol. 466, 2020, doi: 10.1016/j.jsv.2019.115049

[97] H.Q. Guan, K. Feng, K. Yu, Y.L. Cao, Y.H. Wu, *Nonlinear dynamic responses of a rigid rotor supported by active bump-type foil bearings*, Nonlinear Dynamics, vol. 100, iss. 3, pp. 2241–2264, 2020, doi: 10.1007/s11071-020-05608-4

[98] D.E. Bently, T. Hatch'Charles, *Fundamentals of rotating machinery diagnostics*, ASME, 2003.

[99] K. Sim, Y.-B. Lee, T.H. Kim, *Effects of mechanical preload and bearing clearance on Rotordynamic performance of lobed gas foil bearings for oil-free turbochargers*, Tribology Transactions, vol. 56, iss. 2, pp. 224–235, 2013, doi: 10.1080/10402004.2012.737502

[100] Y.B. Lee, S.B. Kwon, T.H. Kim, K. Sim, *Feasibility study of an oil-free turbocharger supported on gas foil bearings via on-road tests of a two-liter class diesel vehicle*, Journal of Engineering for Gas Turbines and Power, vol. 135, iss. 5, 2013, pp. 1-10, doi: 10.1115/1.4007883

[101] J. Park, K. Sim, *A feasibility study of controllable gas foil bearings with piezoelectric materials via rotordynamic model predictions*, Journal of Engineering for Gas Turbines and Power, vol. 141, iss. 2, pp. 1-12, 2018, doi: 10.1115/1.4041384

[102] K. Feng, H.Q. Guan, Z.L. Zhao, T.Y. Liu, *Active bump-type foil bearing with controllable mechanical preloads*, Tribology International, vol. 120, pp. 187–202, 2018, doi: 10.1016/j.triboint.2017.12.029

[103] V. Arora, P.J. van der Hoogt, R.G. Aarts, A. de Boer, *Identification of dynamic properties of radial air-foil bearings*, International Journal of Mechanics and Materials in Design, vol. 6, iss. 4, pp. 305–318, 2010, doi: 10.1007/s10999-010-9137-z

[104] M. Salehi, H. Heshmat, *Frictional dampers dynamic characterization-theory and experiments, Boundary and Mixed Lubrication - Science and Applications*, Proceedings of the 28th Leeds-Lyon Symposium on Tribology, pp. 515–526, 2002, doi: 10.1016/s0167-8922(02)80057-8

[105] M. Salehi, H. Heshmat, J.F. Walton, *On the frictional damping characterization of compliant Bump Foils*, Journal of Tribology, vol. 125, iss. 4, pp. 804–813, 2003, doi: 10.1115/1.1575774

[106] D. Rubio, L. San Andrés, *Bump-type foil bearing structural stiffness: Experiments and predictions*, Journal of Engineering for Gas Turbines and Power, vol. 128, iss. 3, pp. 653–660, 2004, doi: 10.1115/1.2056047

[107] R. Zhou, Y. Gu, G. Ren, S. Yu, *Modeling and stability characteristics of bump-type gas foil bearing rotor systems considering stick–slip friction*, International Journal of Mechanical Sciences, vol. 219, 2022, doi: 10.1016/j.ijmecsci.2022.107091

[108] C. Dellacorte, M.J. Valco, *Load capacity estimation of foil air journal bearings for oil-free turbomachinery applications*, Tribology Transactions, vol. 43, iss. 4, pp. 795–801, 2000, doi: 10.1080/10402000008982410

[109] Y.B. Lee, T.H. Kim, C.H. Kim, N.S. Lee, D.H. Choi, *Dynamic characteristics of a flexible rotor system supported by a viscoelastic foil bearing (VEFB)*, Tribology International, vol. 37, iss. 9, pp. 679–687, 2004, doi: 10.1016/s0301-679x(03)00013-6

[110] Y.B. Lee, T.H. Kim, C.H. Kim, N.S. Lee, D.H. Choi, *Unbalance response of a super-critical rotor supported by foil bearings—comparison with test results©*, Tribology Transactions vol. 47, iss. 1, pp. 54–60, 2004, doi: 10.1080/05698190490279038

[111] Y.B. Lee, T.H. Kim, C.H. Kim, N.S. Lee, *Suppression of subsynchronous vibrations due to aerodynamic response to surge in a two-stage centrifugal compressor with air foil bearings*, Tribology Transactions, vol. 46, iss. 3, pp. 428–434, 2003, doi: 10.1080/10402000308982647

[112] L. San Andrés, D. Rubio, T.H. Kim, *Rotordynamic performance of a rotor supported on bump type foil gas bearings: Experiments and predictions*, Journal of Engineering for Gas Turbines and Power, vol. 129, iss. 3, pp. 850–857, 2006, doi: 10.1115/1.2718233

[113] J.S. Larsen, I.F. Santos, *On the nonlinear steady-state response of rigid rotors supported by air foil bearings—theory and experiments*, Journal of Sound and Vibration, vol. 346, pp. 284–297, 2015, doi: 10.1016/j.jsv.2015.02.017

[114] L. San Andrés, T.H. Kim, *Forced nonlinear response of gas foil bearing supported rotors*, Tribology International, vol. 41, iss. 8, pp. 704–715, 2008, doi: 10.1016/j.triboint.2007.12.009

[115] Z. Guo, Y. Cao, K. Feng, H. Guan, T. Zhang, *Effects of static and imbalance loads on nonlinear response of rigid rotor supported on gas foil bearings*, Mechanical Systems and Signal Processing, vol. 133, 2019, doi: 10.1016/j.ymssp.2019.106271

[116] F. Balducchi, M. Arghir, R. Gauthier, *Experimental analysis of the unbalance response of rigid rotors supported on aerodynamic foil bearings*, Journal of Vibration and Acoustics, vol. 137, iss. 6, 2015, pp. 1-11, doi: 10.1115/1.4031409

[117] J.F. Walton, H. Heshmat, M.J. Tomaszewski, *Testing of a small turbocharger/turbojet sized simulator rotor supported on foil bearings*, Journal of Engineering for Gas Turbines and Power, vol. 130, iss. 3, 2008, pp. 1-7, doi: 10.1115/1.2830855

[118] P. Bonello, M.F.B. Hassan, *An experimental and theoretical analysis of a foil-air bearing rotor system*, Journal of Sound and Vibration, vol. 413, pp. 395–420, 2018, doi: 10.1016/j.jsv.2017.10.036

[119] R. Hoffmann, R. Liebich, *Characterisation and calculation of nonlinear vibrations in gas foil bearing systems–an experimental and numerical investigation*, Journal of Sound and Vibration, vol. 412, pp. 389–409, 2018, doi: 10.1016/j.jsv.2017.09.040

[120] S. Bauman, *An oil-free thrust foil bearing facility design, calibration, and operation*, in 58th Annual Meeting, 28 April - 1 May, 2013, NASA Technical Reports Server (NTRS), 2005.

[121] K. Radil, C. Dellacorte, M. Zeszotek, *Thermal management techniques for oil-free turbomachinery systems*, Tribology Transactions, vol. 50, iss. 3, pp. 319–327, 2007, doi: 10.1080/10402000701413497

[122] H. Heshmat, M.J. Tomaszewski, J.F. Walton, *Small gas turbine engine operating with high-temperature foil bearings*, Turbo Expo: Power for Land, Sea, and Air, vol. 5, pp. 387-393, 2006, doi: 10.1115/GT2006-90791

[123] T.H. Kim, L. San Andrés, *Effect of side feed pressurization on the dynamic performance of gas foil bearings: A model anchored to test data*, Journal of Engineering for Gas Turbines and Power, vol. 131, iss. 1, 2008, pp. 1-8, doi: 10.1115/1.2966421

[124] L. San Andrés, K. Ryu, T.H. Kim, *Thermal management and Rotordynamic performance of a hot rotor-gas foil bearings system—part I: Measurements*, Journal of Engineering for Gas Turbines and Power, vol. 133, iss. 6, 2011, pp. 1-10, doi: 10.1115/1.4001826

[125] L. San Andrés, T.H. Kim, *Thermohydrodynamic analysis of bump type gas foil bearings: A model anchored to test data*, Journal of Engineering for Gas Turbines and Power, vol. 132, iss. 4, pp, 1-10, 2010, doi: 10.1115/1.3159386

[126] T.H. Kim, L. San Andrés, *Thermohydrodynamic model predictions and performance measurements of bump-type foil bearing for oil-free turboshaft engines in rotorcraft propulsion systems*, Journal of Tribology, vol. 132, iss. 2, pp. 1-11, 2009, doi: 10.1115/1.4000279

[127] A. Martowicz, J. Bryła, W.J. Staszewski, M. Ruzzene, T. Uhl, *Nonlocal elasticity in shape memory alloys modeled using peridynamics for solving dynamic problems*, Nonlinear Dynamics, vol. 97, iss. 3, pp. 1911–1935, 2019, doi: 10.1007/s11071-019-04943-5

[128] A. Martowicz, S. Kantor, Ł. Pieczonka, J. Bryła, J. Roemer, *Phase transformation in shape memory alloys: A numerical approach for thermomechanical modeling via peridynamics*, Meccanica, vol. 56, iss. 4, pp. 841–854, 2021, doi: 10.1007/s11012-020-01276-1

[129] A. Martowicz, P. Zdziebko, J. Roemer, G. Żywica, P. Bagiński, *Thermal characterization of a gas foil bearing—a novel method of experimental identification of the temperature field based on integrated thermocouples measurements*, Sensors, vol. 22, iss. 15, pp. 5718, 2022, doi: 10.3390/s22155718

[130] P. Bagiński, G. Żywica, M. Lubieniecki, J. Roemer, *The effect of cooling the foil bearing on dynamics of the rotor-bearings system*, Journal of Vibroengineering, vol. 20, iss. 2, pp. 843–857, 2018, doi: 10.21595/jve.2018.19772

[131] A. Martowicz, J. Roemer, M. Lubieniecki, G. Żywica, P. Bagiński, *Experimental and numerical study on the thermal control strategy for a gas foil bearing enhanced with thermoelectric modules*, Mechanical Systems and Signal Processing, vol. 138, 2022, doi: 10.1016/j.ymssp.2019.106581